DISCRETE AND CONTINUOUS
DYNAMICAL SYSTEMS
Volume **41**, Number **1**, January **2021**

doi:10.3934/dcds.2020215

pp. **87–111**

SOLITARY-WAVE SOLUTIONS OF BENJAMIN-ONO AND OTHER SYSTEMS FOR INTERNAL WAVES. I. APPROXIMATIONS

Jerry L. Bona*

University of Illinois at Chicago
Department of Mathematics, Statistics and Computer Science
851 South Morgan Street, Chicago, IL 60607, USA

Angel Durán

University of Valladolid
Applied Mathematics Department
P/ Belen 15, 47011, Valladolid, Spain

Dimitrios Mitsotakis

Victoria University of Wellington
School of Mathematics and Statistics
PO Box 600, Wellington 6140, New Zealand

Abstract. Considered here are systems of partial differential equations arising in internal wave theory. The systems are asymptotic models describing the two-way propagation of long-crested interfacial waves in the Benjamin-Ono and the Intermediate Long-Wave regimes. Of particular interest will be solitary-wave solutions of these systems. Several methods of numerically approximating these solitary waves are put forward and their performance compared. The output of these schemes is then used to better understand some of the fundamental properties of these solitary waves.

The spatial structure of the systems of equations is non-local, like that of their one-dimensional, unidirectional relatives, the Benjamin-Ono and the Intermediate Long-Wave equations. As the non-local aspect is comprised of Fourier multiplier operators, this suggests the use of spectral methods for the discretization in space. Three iterative methods are proposed and implemented for approximating traveling-wave solutions. In addition to Newton-type and Petviashvili iterations, an interesting wrinkle on the usual Petviashvili method is put forward which appears to offer advantages over the other two techniques. The performance of these methods is checked in several ways, including using the approximations they generate as initial data in time-dependent codes for obtaining solutions of the Cauchy problem.

Attention is then turned to determining speed versus amplitude relations of these families of waves and their dependence upon parameters in the models. There are also provided comparisons between the unidirectional and bidirectional solitary waves. It deserves remark that while small-amplitude solitary-wave solutions of these systems are known to exist, our results suggest the amplitude restriction in the theory is artificial.

2020 *Mathematics Subject Classification.* Primary: 76B55, 76B25; Secondary: 65N35.

Key words and phrases. Internal waves, Benjamin-Ono and Intermediate Long Wave systems, solitary waves, Petviashvili iterative method, pseudospectral methods.

* Corresponding author: Jerry L. Bona.

1. **Introduction.** Field observations and laboratory experiments provide evidence of internal solitary waves in nature (see [43] for an extended review). Such wave motion in the bulk of a fluid occurs because of density stratification. In an idealized situation, where a homogeneous layer of light incompressible fluid rests upon a similar layer of heavier fluid (see Figure 1), and surface tension and diffusion between the two layers as well as damping are ignored, the full equations for internal wave motion are usually taken to be a pair of Euler systems coupled through the interface and with appropriate conditions specified at the lower and upper bounding surfaces.

Just as for surface water waves, in both practical and theoretical situations, it is often fruitful to consider asymptotic approximations of these full equations. There are many asymptotic models in the literature for approximating the propagation of internal waves. Some recent examples are described in [30, 34, 35, 52], but the reader is cautioned that there are many others. The various models depend upon the wave regime, the geometry of the flow domain and the details of the stratification. If the waves are long-crested, so that a one-dimensional description is appropriate, and they are moving mainly in one direction, the extant models include some classical approximations such as the Korteweg-de Vries (KdV) equation, the intermediate long-wave (ILW) equation [44],

$$\zeta_t + (1 + \frac{1}{\delta})\zeta_x + \zeta\zeta_x + \mathbb{T}_\delta \zeta_{xx} = 0,$$

where the parameter $\delta > 0$ depends on the ratio of the depths of the two layers and

$$\mathbb{T}_\delta \zeta = \frac{1}{2\delta} \text{P.V.} \int_{-\infty}^{\infty} \coth\left(\frac{\pi(\xi - x)}{2\delta}\right) \zeta(\xi, t)\, d\xi, \tag{1}$$

and the Benjamin-Ono (BO) equation [16, 53],

$$\zeta_t + \zeta_x + \zeta\zeta_x + \mathbb{H}\zeta_{xx} = 0,$$

where

$$\mathbb{H}\zeta = \frac{1}{\pi} \text{P.V.} \int_{-\infty}^{\infty} \frac{\zeta(\xi, t)}{\xi - x}\, d\xi \tag{2}$$

is the Hilbert transform. The latter equation obtains as a certain deep-water limit in which $\delta \to \infty$ in the ILW equation. In (1) and (2), ζ stands for the small amplitude deviation of the interface between the two fluids of different densities and P.V. denotes the Cauchy Principal Value of the relevant integral. In these highly simplified models, the fluids are taken to be bounded above by a horizontal, impermeable top (the so-called *rigid lid approximation*) and the bottom is either flat and horizontal, or the fluid is taken to be infinitely deep. If the interface is far from the bounding surfaces, the rigid lid approximation is not too bad, but this changes depending upon the geometry of the flow domain and the relative scale of the waves (see [36] for detailed commentary on this point).

A recent formulation in [26] of the Euler equations for the idealized, two-layer situation with a horizontal bottom and the rigid lid condition on the surface involves the Dirichlet-to-Neumann and another nonlocal operator. This formulation lends itself to a systematic derivation of asymptotic models for long-crested internal waves in various regimes. The resulting systems, which include the two studied here, can be extended to more realistic cases with nontrivial bottom topography and a free surface rather than a rigid lid, and with surface tension effects included if the scales require it (see [15] and [39] for examples).

Some of these asymptotic models have been analyzed, theoretically, numerically, or both. The so-called shallow water/shallow water regime, which features long wavelength, but interfacial amplitudes that are allowed to be relatively large with respect to the depth of both fluid layers is studied in [42] and a local well-posedness theory mounted. (The terminology shallow water/shallow water is taken from the paper [26] where the various models are derived. Similar terminology to follow derives from the same source.) The study [42] also includes development of a pseudo-spectral method for approximating solutions of this model along with numerical simulations supporting the local well-posedness results and indicating singularity formation in finite time for certain initial conditions. Linear well-posedness for the systems in the Boussinesq/Boussinesq regime, where the wave amplitude must be small and the wavelength large with respect to the depth of both layers, is in Duchene [39]. Further work in this regime, which included a free surface, is in his later work [40]. This latter paper contains an analysis of the difference between the rigid-lid and the free surface situation as well as an interesting KdV-approximation of the waves. Especially relevant to the present script is work of Xu in [58], who obtains well-posedness results for the ILW/ILW regime where the upper fluid layer is shallow while the interfacial deviations are small with respect to both fluid depths. This paper also justifies rigorously the convergence of the ILW system to the BO system as the depth of the lower layer tends to infinity.

The present essay is devoted to a computational investigation of the model systems that obtain in the BO and ILW regimes. The principal goal of this study is to put forward methods for approximating the solitary-wave solutions of these systems. The existence of small-amplitude solitary-wave solutions of the ILW and BO systems was recently proved in [14]. Other properties of these traveling waves were also studied there. In particular, the solitary waves are shown to decay to zero at infinity exponentially for the the ILW system and quadratically in the case of the BO system. The present paper is focused on the numerical generation of the solitary-wave profiles of both systems. This is of interest in its own right, but it will be especially helpful in a companion paper [25] which will examine dynamic properties of the solitary-wave solutions obtained in the present work.

Three iterative techniques are presented for the numerical generation of solitary waves, namely, the Petviashvili method [55], an extended fixed-point algorithm based on the Petviashvilli method put forward in [9] and a Conjugate Gradient Newton method [59]. The outcomes of using the three schemes are examined and found to be almost identical, another indication that they are producing accurate approximations. Once there is in hand reliable approximations, a variety of the solitary waves' more detailed properties, such as their shape and their speed-amplitude relation are discussed. A comparison between the solitary-wave solutions of unidirectional models of ILW and BO type and those of the associated systems is also undertaken.

The structure of the paper is as follows. In Section 2, the ILW and BO systems derived in [26] are introduced and some fundamental properties of the initial-value problem for both the full (2-space dimensional) and the long-crested (1-dimensional) versions are recalled. Also introduced are the unidirectional versions of these models. These are obtained formally by a standard procedure. They lead to equations similar to, but not identical with the usual BO and ILW equations. The traveling-wave solutions of the unidirectional models will later be compared with those of the systems. Section 3 is devoted to the numerical computation of solitary-wave

solutions using the three iterative techniques mentioned earlier. The fact that the computed profiles are accurate approximations of traveling waves is confirmed in two ways. First, the convergence of the iterations is analyzed by computing the norm of the difference between two consecutive iterations and the norm of the residual error. Second, when the generated profiles are used as initial data for a fully discrete numerical scheme for the time-dependent systems, we check whether or not the resulting time-dependent solutions appears to be a traveling wave. We also check that the approximations behave properly under grid refinement. Comparisons of the approximate solitary waves of the BO and ILW systems are also made with the solitary-wave solutions of associated unidirectional models in Section 4. As already mentioned, the more detailed dynamics of these solitary wave solutions will be reported in the second part of this study.

The conclusions drawn from our study do not reveal marked difference between the BO-regime and the ILW-regime. To save space and avoid repetitive material, we have chosen to focus more upon the BO systems. Commentary and a few select details for the ILW systems are put in where they are warranted.

2. **Mathematical models for internal waves.** The model equations that are the central focus of attention are introduced here.

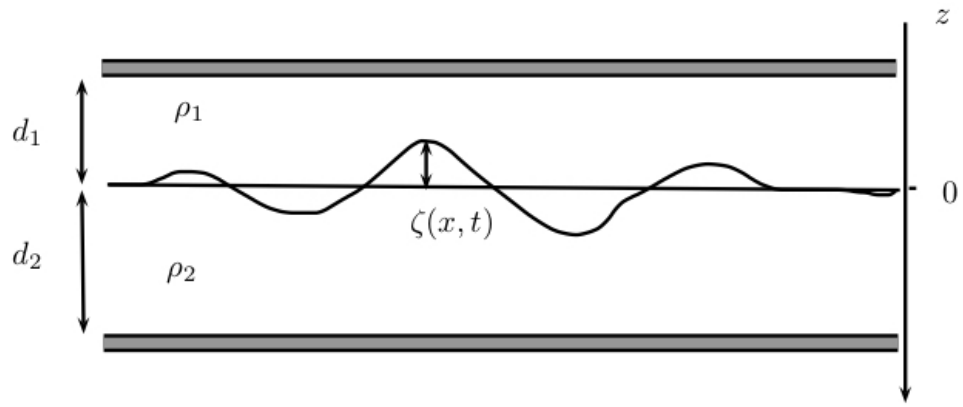

FIGURE 1. Sketch of an ideal fluid system for internal wave propagation. The fluid layers are homogeneous with densities $\rho_1 < \rho_2$.

2.1. **The Benjamin-Ono (BO) and Intermediate Long-Wave (ILW) systems.** The BO and the ILW systems are asymptotic models for internal waves propagating along the interface of a two-layer system of fluids. Assuming that the interfacial surface and the horizontal velocity are both graphs over the featureless bottom, they were derived in [26] for the description of wave motion in particular scaling regimes. The asymptotic derivation starts with the two-layer Euler system of equations that is taken as a more complete rendition of the idealized situation sketched in Figure 1. This idealized configuration consists of two inviscid, homogeneous fluids of depths d_j and densities ρ_j, $j = 1, 2$, with $\rho_2 > \rho_1$ for static stability. The upper layer is taken to be bounded above by a horizontal rigid lid (the top is an impenetrable bounding surface) while the lower layer is bounded below by an impermeable, horizontal, flat bottom (ILW case) or is infinitely deep (BO case).

The deviation of the interface from its rest position, denoted by ζ, is assumed to be a graph over the bottom (in one or two spatial dimensions) and surface tension at the interface and diffusion across it are ignored.

The derivation in [26] is based on a reformulation of the Euler system that involves two nonlocal operators, a standard Dirichlet-to-Neumann operator and an interfacial operator that relates the velocity potentials in the two layers. This reformulation of the problem lends itself to the analysis of different asymptotic regimes. Models for the various regimes are obtained by expanding the non-local operators with respect to suitable small parameters. These parameters mainly depend on the amplitude and wavelength of the motion and the depth ratio of the two layers. Among the many physical regimes that can be obtained with this approach, the systems considered here correspond to the assumptions that the interfacial wave is of small amplitude with respect to the upper fluid layer, which in turn is assumed to be shallow with respect to the wavelength. In the ILW regime, the amplitude of the interface is also small compared to the depth of the lower layer, while in the BO regime the lower layer is taken to be of infinite depth (i.e. $d_2 = \infty$). These systems both take the form

$$\begin{aligned} \left[1 + \sqrt{\mu}\frac{\alpha}{\gamma}\mathcal{H}\right]\partial_t\zeta + \frac{1}{\gamma}\nabla\cdot\left((1-\varepsilon\zeta)\mathbf{v}\right)_x - (1-\alpha)\frac{\sqrt{\mu}}{\gamma^2}\mathcal{H}\nabla\cdot\mathbf{v} = 0, \\ \partial_t\mathbf{v} + (1-\gamma)\nabla\zeta - \frac{\varepsilon}{2\gamma}\nabla|\mathbf{v}|^2 = 0, \end{aligned} \tag{3}$$

where the gradient ∇ and the divergence $\nabla\cdot$ are taken in the horizontal variables x, y in a standard Cartesian coordinate system in which the vertical variable z increases in the direction opposite to which gravity acts. In (3), $\gamma = \rho_1/\rho_2 < 1$ is the density ratio while $\varepsilon = a/d_1$ and $\mu = d_1^2/\lambda^2$ where a is a typical wave amplitude and λ a typical wavelength. The non-dimensional parameters ϵ and μ are assumed to be small compared to one, corresponding to assuming the wave motion has small amplitude and long-wavelength with regard to the depth of the upper fluid. The parameter α is a modeling parameter which arises from the use of a BBM-type remodeling of the dispersion (see [18], [26], [23]). It subsists on the lower-order relation

$$\gamma\zeta_t \;=\; -\nabla\cdot\mathbf{v} + \text{ higher}-\text{order terms},$$

which formally implies that

$$\frac{\sqrt{\mu}}{\gamma}\mathcal{H}\zeta_t \;=\; -\frac{\sqrt{\mu}}{\gamma^2}\mathcal{H}\nabla\cdot\mathbf{v} + \text{ negligible}-\text{order terms}.$$

In principle, α can take any real value without changing the formal level of approximation. However, the initial-value problem is not linearly well-posed unless $\alpha \geq 1$. In both BO and ILW regimes, $\mu \sim \varepsilon^2 \ll 1$ is assumed. The system (3) involves the interfacial deviation ζ and the quantity

$$\mathbf{v} := \mathbf{H}^{\mu,0}[\varepsilon\zeta]\psi - \gamma\nabla\psi,$$

which is a kind of horizontal velocity variable; ψ is the trace on the interfacial free surface of the velocity potential associated with the upper fluid and $\mathbf{H}^{\mu,0}$ an interfacial operator that links the two velocity potentials in the case of a lower layer of infinite depth. Finally, $\mathcal{H}$ is a nonlocal Fourier multiplier operator given in terms of its symbol as $\widehat{\mathcal{H}f}(\mathbf{k}) = g(\mathbf{k})\widehat{f}(\mathbf{k})$ where

$$g(\mathbf{k}) = \begin{cases} |\mathbf{k}| & \text{in the BO case,} \\ |\mathbf{k}|\coth(\sqrt{\mu_2}|\mathbf{k}|) & \text{in the ILW case,} \end{cases} \tag{4}$$

for wavenumbers $\mathbf{k} \in \mathbb{R}^2$. A circumflex adorning a function f denotes that function's Fourier transform with respect to the spatial variable and $\mu_2 = d_2^2/\lambda^2$ is of order 1, as mentioned previously.

If the wave motion in question is long-crested, then there is a preferred axis of propagation, taken here to be the x-direction, and variations along the crest in the y-direction can be ignored at this level of approximation. In this case, the y-component of the 'velocity' $\mathbf{v}$ is zero and all derivatives with respect to the y-variable can be ignored. One of the three equations in (3) is then trivially satisfied and the other two devolve to a one-dimensional system,

$$\begin{aligned} &\left[1 + \sqrt{\mu}\frac{\alpha}{\gamma}\mathcal{H}\right]\zeta_t + \frac{1}{\gamma}\left((1-\varepsilon\zeta)u\right)_x - (1-\alpha)\frac{\sqrt{\mu}}{\gamma^2}\mathcal{H}u_x = 0, \\ &u_t + (1-\gamma)\zeta_x - \frac{\varepsilon}{2\gamma}(u^2)_x = 0, \end{aligned} \tag{5}$$

where u is a horizontal velocity-like variable. Here, $\mathcal{H}$ is a one-dimensional Fourier multiplier operator with symbol $g(k)$ given by (4) with $\mathbf{k} = (k, 0)$, or what is the same, $\mathcal{H} = \partial_x \mathbb{T}_{\sqrt{\mu_2}}$ with $\mathbb{T}_{\sqrt{\mu_2}}$ given by (1) in the case of the ILW system and $\mathcal{H} = \partial_x \mathbb{H}$ with $\mathbb{H}$ given by (2) for the BO system.

2.2. **Mathematical properties.** Reviewed in this subsection are some of the more important mathematical features of the system (3). First, the well-posedness of these models deserves comment. The linear dispersion relations for them are easily derived. If $\omega = \omega(k)$ is the frequency associated to the one-dimensional wavenumber k, then

$$\omega(k) \;=\; \pm k\sqrt{\frac{1-(1-\alpha)g(k)}{1+\sqrt{\mu}\dfrac{\alpha}{\gamma}g(k)}}\,.$$

From this calculation, one can extract conclusions analogous to those appearing in [30, 48, 51], which is that linear well-posedness of (5) obtains if and only if $\alpha \geq 1$.

Indeed, Xu [58] studied the well-posedness of this ILW system when $\alpha > 1$ for both the 1-dimensional and 2-dimensional cases. His analysis allowed for a free surface, but specialized to the rigid lid situation, he obtained local well-posedness in lower-order Sobolev spaces on the short time-scale $O(\sqrt{\mu}) = O(\varepsilon)$ and in higher-order Sobolev spaces on the much longer time scale $O(1/\sqrt{\mu}) = O(1/\varepsilon)$. The convergence of the solutions of the ILW system to those of the BO system was also shown in the same paper, thereby suggesting that similar well-posedness results hold for the BO system when $\alpha > 1$.

In consequence of Xu's results and the linear ill-posedness conclusion posited earlier when $\alpha < 1$, it will be presumed henceforth that $\alpha > 1$ and that solutions corresponding to smooth, localized initial data obtain and continue to be smooth and localized, at least over some positive time interval. This is sufficient to rigorously justify the time-dependent numerical approximations put forward later in this essay.

Nonlinear, dispersive wave equations often have invariant functionals, which is to say, functionals which, when evaluated on solutions of the system, do not vary with time. The present systems have the simple invariants

$$I_1(\zeta, u) = \int_{-\infty}^{\infty} \zeta \; dx, \quad I_2(\zeta, u) = \int_{-\infty}^{\infty} u \; dx, \tag{6}$$

which are time-independent when evaluated on smooth solutions that decay appropriately to zero at $\pm\infty$. The invariance of I_1 can be interpreted as conservation of

mass. On the other hand, the quantities

$$I = \int_{-\infty}^{\infty} \zeta u \, dx \qquad \text{and}$$
$$H = \frac{1-\gamma}{2}\int_{-\infty}^{\infty} \zeta^2 \, dx - \frac{\varepsilon}{2\gamma}\int_{-\infty}^{\infty} \zeta u^2 \, dx + \frac{1}{2\gamma}\int_{-\infty}^{\infty} u^2 \, dx - (1-\alpha)\frac{\sqrt{\mu}}{2\gamma^2}\int_{-\infty}^{\infty} u\mathcal{H}u \, dx,$$

which roughly correspond to momentum and energy, are not necessarily time-independent, *viz.*

$$\frac{d}{dt}I = -\frac{\alpha\sqrt{\mu}}{\gamma}\int_{-\infty}^{\infty} u\mathcal{H}\zeta_t \, dx \quad \text{and}$$
$$\frac{d}{dt}H = -\frac{\alpha\sqrt{\mu}}{\gamma}\int_{-\infty}^{\infty}\left((1-\gamma)\zeta - \frac{\varepsilon}{2\gamma}u^2\right)\mathcal{H}\zeta_t \, dx.$$

They are preserved by the flow induced by (5) only when $\alpha = 0$. In this case, H is a Hamiltonian for the system, as observed already in [36]. (However, in this case the system (5) is not linearly well-posed. Indeed, using the method employed in [12] to show the Kaup system for surface waves is ill posed, one can show that the full nonlinear system (5) is ill-posed in smooth function spaces. This point is not developed here.) So far as we are aware, the system (5) has only the very simple conservation laws displayed in (6) for $\alpha \neq 0$.

Next, attention is turned to the existence of solitary-wave solutions. These will be traveling-wave solutions $\zeta(x,t) = \zeta(x - c_s t)$, $u(x,t) = u(x - c_s t)$ of (5), moving with constant speed c_s, whose profiles tend to 0 as $x \to \pm\infty$. After one integration, the system (5) implies that the profiles $\zeta(X), u(X), X = x - c_s t$, satisfy the system

$$\begin{pmatrix} -c_s\left(1 + \dfrac{\sqrt{\mu}\alpha}{\gamma}\,\mathcal{H}\right) & \dfrac{1}{\gamma} + (\alpha-1)\dfrac{\sqrt{\mu}}{\gamma^2}\,\mathcal{H} \\ 1-\gamma & -c_s \end{pmatrix}\begin{pmatrix}\zeta \\ u\end{pmatrix} = \frac{\varepsilon}{\gamma}\begin{pmatrix}\zeta u \\ \frac{1}{2}u^2\end{pmatrix}. \tag{7}$$

The second equation in (7) is quadratic in u which immediately implies two interesting properties. First, since u is real, the discriminant must be nonnegative, which leads to a lower bound for the profile ζ, specifically,

$$d = c_s^2 + 2\varepsilon c_\gamma^2 \zeta \geq 0 \quad \Rightarrow \quad \zeta \geq -\frac{c_s^2}{2\varepsilon c_\gamma^2},$$

where

$$c_\gamma = \sqrt{(1-\gamma)/\gamma}; \tag{8}$$

remember, $\gamma < 1$ because the quiescent system is assumed to be statically stable. A second consequence is that the deviation ζ of the free interface can be solved in terms of the velocity u and this can be used to reduce the system (7) to a single equation for u, namely

$$\left[-c_s^2\left(1 + \frac{\alpha\sqrt{\mu}}{\gamma}\mathcal{H}\right) + c_\gamma^2\left[1 + (\alpha-1)\frac{\sqrt{\mu}}{\gamma}\mathcal{H}\right]\right]u = \frac{c_s\varepsilon}{2\gamma}\left(3 + \frac{\alpha\sqrt{\mu}}{\gamma}\mathcal{H}\right)u^2 + \frac{\varepsilon^2}{2\gamma^2}u^3. \tag{9}$$

Once u is determined, ζ may be obtained from the formula

$$\zeta = \frac{1}{1-\gamma}\left(c_s u + \frac{\varepsilon}{2\gamma}u^2\right).$$

Note that if (c_s, ζ, u) is a solution of (9) then $(-c_s, \zeta, -u)$ is also a solution with the same profile, but traveling in the opposite direction.

The corresponding system for the Fourier transform of the profiles is

$$\begin{pmatrix} -c_s\left(1+\frac{\sqrt{\mu}\alpha}{\gamma}g(|k|)\right) & \frac{1}{\gamma}+(\alpha-1)\frac{\sqrt{\mu}}{\gamma^2}g(|k|) \\ 1-\gamma & -c_s \end{pmatrix} \begin{pmatrix} \widehat{\zeta}(k) \\ \widehat{u}(k) \end{pmatrix} = \frac{\varepsilon}{\gamma} \begin{pmatrix} \widehat{\zeta u}(k) \\ \widehat{\left(\frac{1}{2}u^2\right)}(k) \end{pmatrix} \tag{10}$$

for wavenumbers $k \in \mathbb{R}$, where $g(k) = g(\mathbf{k})$ is as in (4) with $\mathbf{k} = (k, 0)$.

Assuming the right-hand side is known, this linear system may be "solved". Taking the inverse Fourier transform of the result leads to a system of convolution equations of the general form

$$\begin{aligned} \zeta &= k_{11} * (\zeta u) + \frac{1}{2}k_{12} * \left(u^2\right) + \frac{1}{2}m_{12} * \left(\mathcal{H}u^2\right), \\ u &= k_{21} * (\zeta u) + \frac{1}{2}k_{22} * \left(u^2\right) + \frac{1}{2}m_{22} * \left(\mathcal{H}u^2\right), \end{aligned}$$

for some kernel functions k_{ij}, m_{ij}, $i, j = 1, 2$. The latter formulation could be useful in proving existence of the solitary-wave solutions, *e.g.* by use of techniques such as described in [16, 17, 22, 27, 56], but this is not pursued here. The iterative methods used here to obtain approximations to solitary waves will rely upon the formulations (9) and (10). Note that the solitary-wave solutions of both the ILW and BO systems that are shown to exist in [14] were obtained via the implicit function theorem, so being limited to small amplitudes.

2.3. **Unidirectional regularized BO and ILW equations.** Going back to the 19^{th} century in the work of Boussinesq in the 1870's, it was known how to formally reduce two-way models to corresponding unidirectional models. A good account of the classical theory can be found in Whitham's text [57]. Rigorous theory justifying the classical formal reduction of the two-way surface water wave models to unidirectional models may be found in [2]. However, no such theory is currently available for the ILW and BO systems being considered here.

An indication of the application of the classical approach to deriving unidirectional models as it applies to the ILW and BO systems is now described. The important first observation is that if higher-order terms are neglected, these models come down to a factorized version of the linear wave equation. The solution consists of waves moving to the left and to the right at speed c_γ (see (8)). Once the waves have separated, the right- and left-propagating waves no longer interact and one expects that a pair of unidirectional models could approximate their further evolution. For waves moving to the right, say, this results in $u = \zeta$ and $\zeta_t + c_\gamma \zeta_x = 0$. The decomposition into right and left moving waves can be made exactly for the linear system obtained from (5) by simply dropping the quadratic terms, but this appears not to be the case when nonlinearity is present (compare with the discussion in [21]). Without going into details, which follow very much as in the paper [2] on Boussinesq systems for surface water waves mentioned above, the way forward is to consider higher-order corrections to u of the form

$$u = \sqrt{\gamma(1-\gamma)}\,(\zeta + A\varepsilon + B\sqrt{\mu}), \tag{11}$$

with A and B to be determined as functions of ζ. Substituting (11) into the system (5), ignoring all terms of higher order than linear in ϵ and $\sqrt{\mu}$ and demanding the resulting two equations be consistent yield $A = \frac{1}{4}\zeta^2$ and $B = \frac{1}{2\gamma}\mathcal{H}\zeta$, and so to a

single unidirectional equation for ζ, namely

$$\left[1+\sqrt{\mu}\frac{\alpha}{\gamma}\mathcal{H}\right]\zeta_t+c_\gamma\zeta_x-\varepsilon\frac{3}{4}c_\gamma(\zeta^2)_x-\frac{\sqrt{\mu}}{2\gamma}c_\gamma(1-2\alpha)\mathcal{H}\zeta_x=0. \tag{12}$$

By taking $\alpha=0$ in (12) and the appropriate choice of the operator $\mathcal{H}$, the original versions of the BO and ILW equations are recovered as in [33] and [45] (see [36] for more details). If instead, $\alpha=1/2$, then the regularized or BBM version of these equations emerges, as described in [47]. Note, however, that for neither $\alpha=0$ nor $\alpha=1/2$ is the two-way model well posed. The model (12), which varies with the choice of α, will be referred to as the rBO or rILW equation, depending upon which operator $\mathcal{H}$ is being discussed. As remarked, there is no theory comparing solutions of this model and the associated solutions of the systems in (5) as in the theory developed in [2] for surface waves. However, the comparisons made of the solitary-wave solutions of the system versus those of the the pertinent unidirectional model in Section 4 provide some hope that such a result may in fact be true. Part of our companion paper [25] will deal with this issue in a dynamical setting.

Local well-posedness for the equations displayed in (12) holds in the L_2-based Sobolev spaces $H^s(\mathbb{R})$ for any $\alpha\geq 0$ and $s\geq 3/2$. Theorem 1 in [3] suffices for our purposes, though sharper results have since been obtained. As our simulations all feature smooth initial data, superior results are not needed here. As far as the dependence of the unidirectional models on the parameter α is concerned, a comparison between model equations for nonlinear dispersive long waves of KdV type and associated regularized versions, which include both the ILW and BO cases, was carried out in [3] (see the related work in [6], [46] and [47]). A more systematic comparison between KdV-type equations when the nonlinearity and dispersion are varied appears in [28]. The upshot of these studies is that over time scales of order $O(1/\epsilon)$, small variations in the choice of α do not make a lot of difference.

The unidirectional equation (12) has the conservation laws

$$C(\zeta)=\int_{-\infty}^{\infty}\zeta dx,\qquad D(\zeta)=\frac{1}{2}\int_{-\infty}^{\infty}\left(\zeta^2+\sqrt{\mu}\frac{\alpha}{\gamma}\zeta\mathcal{H}\zeta\right)dx,$$
$$E(\zeta)=\frac{c_\gamma}{2}\int_{-\infty}^{\infty}\left(\zeta^2-\sqrt{\mu}\frac{(1-2\alpha)}{2\gamma}\zeta\mathcal{H}\zeta-\frac{1}{2}\zeta^3\right)dx.$$

For $\alpha\geq 0$, these are helpful in deducing global in time well-posedness for the models, a conclusion not established for the system (5). They are also helpful in tracking the accuracy of numerical schemes; if one of these functionals is applied to an approximate solution, then its temporal variation provides an indication of how well the scheme is adhering to the exact solution. The functional E furnishes a Hamiltonian structure for these equations, but this is not needed in the present discussion.

Finally, we mention that for the family of equations (12) where the operator $\mathcal{H}$ is of Benjamin-Ono type, a simple rescaling of the results in [47] shows that there are exact solitary-wave solutions $\zeta(x,t)=\zeta(x-c_st)$ having the form,

$$\zeta(\xi)=\frac{AB^2}{\xi^2+B^2}, \tag{13}$$

with

$$A=\frac{8}{3\varepsilon}\frac{c_\gamma-c_s}{c_\gamma}\quad\text{and}\quad|B|=\frac{\sqrt{\mu}}{2\gamma}\frac{2\alpha c_s+(1-2\alpha)\,c_\gamma}{c_\gamma-c_s}. \tag{14}$$

When $\alpha = 0$, the solitary-wave solutions of the usual BO equation are recovered. These are known to be stable and unique, up to spatial translations (see [19] and [13]). A similar analysis as that appearing in [19] shows the solitary-wave solutions of the rBO-equation are also stable. When $\mathcal{H}$ in (12) has the ILW symbol, there are also exactly known solitary-wave solutions, namely

$$\zeta(\xi) = \frac{a\sin(a\sqrt{\mu_2})}{\cosh(a\xi) + \cos(a\sqrt{\mu_2})}\ , \tag{15}$$

where a is the unique solution of

$$a\sqrt{\mu_2}\cot(a\sqrt{\mu_2}) = 1 - (1+c_s)\sqrt{\mu_2} \quad \text{with} \quad a \in (0, \pi/\sqrt{\mu_2}). \tag{16}$$

Unlike their BO counterparts, these decrease to zero at an exponential rate as the spatial variable becomes large [7, 33, 44, 45]. They, too, are stable and unique (see [4] and [7]). A bit of further analysis together with rescaling allows one to conclude the same for the rILW equation. With appropriate scaling, the limit $\mu_2 \to \infty$ recovers BO solitary waves, while the limit $\mu_2 \to 0$ leads to KdV solitary waves (see [33] and [45]).

3. **Numerical approximation of solitary waves.** In this section, iterative methods are developed to approximate traveling-wave solutions of the equations under study. Strong evidence is developed that there are indeed large amplitude solitary-wave solutions for the ILW and BO systems, just as there are for the unidirectional models.

As solitary waves decay rapidly to zero away from their peak, it has become common practice to approximate them by way of a related periodic problem posed on a sufficiently large period domain $(-l, l)$. That this actually works is born out by experience, but there is theory justifying it in particular cases, *e.g.* [17], [20], [32] and the references contained therein. This approach will be followed here. Recall that in the periodic case, the corresponding Hilbert transform acting on $2l-$periodic functions f can be represented by

$$\mathbb{H}_l f(x) = \frac{1}{2l}\text{P.V.}\int_{-l}^{l} \cot\left(\frac{\pi(x-y)}{2l}\right) f(y)dy,$$

while in the ILW case, the periodic version of the operator $\mathbb{T}_\delta$ is given in terms of the Fourier series

$$\mathbb{T}_\delta f(x) = i\sum_{k\in\mathbb{Z}^*} \coth\left(\frac{k\pi\delta}{l}\right)\widehat{f}(k)e^{ik\frac{\pi}{l}x},$$

where $\widehat{f}(k)$ denotes the $k-$th Fourier coefficient of f and $\mathbb{Z}^* = \mathbb{Z}\setminus\{0\}$ (see [1]).

The periodic perspective leads naturally to the use of finite Fourier series to provide approximations. The first step is to rescale the period domain by way of the simple change of variables $x \hookrightarrow \pi x/\ell$ that maps $[-\ell, \ell]$ to $[-\pi, \pi]$. This alters the symbol g of the operator $\mathcal{H}$ appearing in (10) and (9), but does not change its basic structure (the new symbol is $g(\pi k/\ell)$). For $N \geq 1$, consider the finite-dimensional space $S_N = \text{span}\{e^{\mathrm{i}kx} : k \in \mathbb{Z},\ -N \leq k \leq N\}$. Given the Fourier nodes $x_j = (j-N)\pi/N$, $j = 0, \ldots, 2N$, and given u and v in S_N, define the inner product $\langle u, v\rangle = \frac{2\pi}{2N+1}\sum_{j=0}^{2N} u(x_j)\overline{v(x_j)}$. The *discrete Fourier coefficients* of u are then $\hat{u}_k = \frac{1}{2N+1}\sum_{j=0}^{2N} u(x_j)e^{-\mathrm{i}kx_j}$, $k = -N, \cdots, N$ and the approximation of a

periodic function u on $[-\ell,\ell]$ is the usual finite Fourier series

$$u(x) = \sum_{k=-N}^{N} \widehat{u}_k e^{i\frac{k\pi x}{\ell}}.$$

3.1. **The Petviashvili method.** Three iterative numerical methods for the computation of approximate solitary-wave profiles for the system (5) are considered. The first is the well known Petviashvili scheme [55]. A brief description of this method in our context follows.

Note first that the system (7) for the putative solitary-wave profiles contains nonlinearities that are homogeneous functions of the variables ζ and u of degree two. Consider a classical fixed-point algorithm

$$\begin{aligned} &\mathcal{L}U_{n+1} = \mathcal{N}(U_n), \quad n = 0,1,\cdots, \text{ with } \mathcal{N}(U) = \mathcal{N}(\zeta,u) = \frac{\varepsilon}{\gamma}\begin{pmatrix}\zeta u\\ \frac{1}{2}u^2\end{pmatrix}\\ &\text{and} \quad \mathcal{L} = \begin{pmatrix} -c_s\left(1+\dfrac{\sqrt{\mu}\alpha}{\gamma}\,\mathcal{H}\right) & \dfrac{1}{\gamma}+(\alpha-1)\dfrac{\sqrt{\mu}}{\gamma^2}\,\mathcal{H}\\ 1-\gamma & -c_s\end{pmatrix}, \end{aligned} \tag{17}$$

for the iterative resolution of (7), where $U_n = (\zeta_n, u_n)^T$. This will not converge in general. The reason for this is that the corresponding iteration matrix has the degree of homogeneity of $\mathcal{N}$, which is two, as an eigenvalue, thereby indicating divergence of general initial guesses. The Petviashvili modification introduces a stabilizing factor to get around this problem. In detail, the modified procedure consists of defining

$$\begin{aligned} &M_n = \frac{\langle \mathcal{L}U_n, U_n\rangle}{\langle \mathcal{N}(U_n), U_n\rangle}, \quad \text{and then using the iteration}\\ &\mathcal{L}U_{n+1} = M_n^2\mathcal{N}(U_n), \quad n = 0,1,\cdots. \end{aligned} \tag{18}$$

The stabilizing factor M_n^2 acts as filter on the spectrum of the iteration matrix of the classical fixed-point algorithm, removing the eigenvalue associated to the degree of homogeneity and preserving the rest of the spectrum (see [10]). This property will be illustrated below.

Our implementation of the Petviashvili iteration is applied to the formulation (10) in terms of the Fourier components of ζ and u. Let $Z = (Z_{-N},\cdots,Z_p,\cdots,Z_N)$ and $U = (U_{-N},\cdots,U_p,\cdots,U_N)$ be the Fourier components of the approximations in S_N of ζ and u, respectively. Then the equation

$$\begin{pmatrix} -c_s\left(1+\dfrac{\sqrt{\mu}\alpha}{\gamma}\,g(|k_p|)\right) & \dfrac{1}{\gamma}+(\alpha-1)\dfrac{\sqrt{\mu}}{\gamma^2}\,g(|k_p|)\\ 1-\gamma & -c_s\end{pmatrix}\begin{pmatrix}Z_p\\ U_p\end{pmatrix} = \frac{\varepsilon}{\gamma}\begin{pmatrix}(Z*U)_p\\ \frac{1}{2}(U*U)_p\end{pmatrix},$$

is imposed for $-N \le p \le N$, where $k_p = i\pi p/\ell$, the symbol g is as in (4) with $\mathbf{k} = (k,0)$ and $*$ denotes the periodic convolution in $\mathbb{R}^{2n+1}$. In this form, the iteration (18) requires the solution of a 2×2 system of nonlinear equations for each Fourier component of the numerical approximation. In practice, the periodic convolutions on the right-hand side are carried out by using the fast Fourier transform (FFT) as in [41].

3.2. **The e-Petviashvili method.** A modification of the classical Petviashvili method leads to an interesting extended version of the basic idea. It is here used to solve the equation (9) for the u profile instead of the system (7). The method is applied to the equation written in the form

$$\begin{aligned} &\mathcal{L}u = \mathcal{N}_1(u) + \mathcal{N}_2(u), \quad \text{where} \\ &\mathcal{L} = \left[c_s^2\left(1 + \frac{\alpha\sqrt{\mu}}{\gamma}\mathcal{H}\right) - c_\gamma^2\left(1 + (\alpha-1)\frac{\sqrt{\mu}}{\gamma}\mathcal{H}\right)\right], \\ &\mathcal{N}_1(u) = \frac{c_s\varepsilon}{2\gamma}\left(3 + \frac{\alpha\sqrt{\mu}}{\gamma}\mathcal{H}\right)u^2 \ \text{ and } \ \mathcal{N}_2(u) = \frac{\varepsilon^2}{2\gamma^2}u^3. \end{aligned} \tag{19}$$

This equation contains nonlinearities homogeneous of degree two and three. The idea here is the same as for the standard Petviashvili method, namely to filter out the unstable eigenvalues with stabilizing factors. Because of the mixed homogeneity, different powers of the stabilizing factor are attached to the two nonlinearities (see [9, 54]). The resulting scheme will be referred to as the e-Petviashvili method. In detail, it has the form

$$\begin{aligned} &M_n = \frac{\langle \mathcal{L}u_n, u_n\rangle}{\langle \mathcal{N}_1(u_n) + \mathcal{N}_2(u_n), u_n\rangle}, \ \text{coupled with the iteration} \\ &\mathcal{L}u_{n+1} = M_n^2\mathcal{N}_1(u_n) + M_n^{3/2}\mathcal{N}_2(u_n), \quad n = 0, 1, \dots \ . \end{aligned} \tag{20}$$

If the procedure succeeds, then the final iterate for the approximation of u can be used to obtain an approximation to the ζ-profile via formula (9). The implementation is via the FFT just as for the standard Petviashvili method described above.

3.3. **The Conjugate-Gradient-Newton method.** The third iterative method considered here is the standard Conjugate-Gradient-Newton (CGN) method. As in the case of the e-Petviashvili method, the CGN method is applied to the equation (9) written in the form

$$F(u) = \mathcal{L}u - \mathcal{N}_1(u) - \mathcal{N}_2(u) = 0,$$

where $\mathcal{L}$, $\mathcal{N}_1$ and $\mathcal{N}_2$ are defined in (19). The $(n+1)^{st}$ iterate is obtained from the n^{th} by the Newton procedure,

$$F_n'(u_n)\Delta u_n = -F(u_n), \tag{21}$$

$$u_{n+1} = u_n + \Delta u_n. \tag{22}$$

The operator F' is the usual Fréchet derivative

$$F'(u)v = \mathcal{L}v - \frac{c_s\varepsilon}{\gamma}\left(3 + \frac{\alpha\sqrt{\mu}}{\gamma}\mathcal{H}\right)(uv) - \frac{3\varepsilon^2}{2\gamma^2}u^2v \ ,$$

of F. Due to the translational invariance of the equation, $F'(u)$ is always singular. Consequently, the system (21) is ill-conditioned. Following [49, 59], this problem can be obviated by use of preconditioning operators of the form $M = z - \partial_x^2$ for an appropriate value of the parameter z. On the other hand, the computation of the Jacobian is avoided by using a conjugate gradient implementation of (21). Thus, the technique contains a coupled pair of iterative processes, an inner one for the resolution of the system for the increments Δu_n and an outer one that advances to the next level of approximation via (22). The reader may consult [38] for more discussion and other alternatives. As in the two previous algorithms, the computations are carried out in the Fourier space with the same discrete operators. Once

(21) and (22) lead to the final approximation to the u-profile, an approximation of ζ is obtained by use of (9) as in the case of the e-Petviashvili method.

3.4. **Accuracy of the iterative methods.** Presented here is a set of numerical experiments that compare the accuracy and performance of the three iterative schemes designed to generate approximations of solutions of (7). To get started, a good initial guess is needed. One choice is to use the analytic solitary-wave solutions in formulas (13)-(14) for the unidirectional rBO equation or in (15)-(16) for the rILW equation. Another possible initial approximation can be obtained by linearizing the second equation in (7) to obtain

$$\begin{aligned} &-c_s\left[1+\tfrac{\sqrt{\mu}\alpha}{\gamma}\mathcal{H}\right]\zeta+\tfrac{1}{\gamma}u-\tfrac{\varepsilon}{\gamma}\zeta u-(1-\alpha)\tfrac{\sqrt{\mu}}{\gamma^2}\mathcal{H}u=0,\\ &-c_s u+(1-\gamma)\zeta=0.\end{aligned}$$

Solving the second equation in the last display for u, to wit,

$$u=\frac{1-\gamma}{c_s}\zeta, \tag{23}$$

and substituting this into (23) yields

$$\frac{c_\gamma^2-c_s^2}{c_s}\zeta-\frac{\varepsilon\, c_\gamma^2}{c_s}\zeta^2-\frac{\sqrt{\mu}(\alpha c_s^2+(1-\alpha)c_\gamma^2)}{c_s\gamma}\mathcal{H}\zeta=0. \tag{24}$$

Equation (24) can be solved analytically and then u determined from (23), leading to formulas similar to those for the solitary-wave solution of the corresponding unidirectional equation. For example, in the case of the BO system, the solution of (24) takes the form (13) with

$$A=\frac{2}{\varepsilon}\frac{c_\gamma^2-c_s^2}{c_\gamma^2}\quad\text{and}\quad |B|=\frac{\sqrt{\mu}}{\gamma}\cdot\frac{\alpha c_s^2+(1-\alpha)c_\gamma^2}{c_s^2-c_\gamma^2}.$$

Notice that when $c_s>c_\gamma$, these solutions are negative. In any event, the latter formula and its ILW counterpart are the ones used as initial guesses to start all three algorithms. It transpires that this choice leads to convergence of the iterations in a sufficiently robust way so as not to require alternative approaches, such as numerical continuation or acceleration techniques (see [5] and [11], respectively).

The iterative procedures are stopped when either the L_∞-norm of the difference between two consecutive iterations or the L_∞-norm of the residual error given by

$$RE_n=\left\|\mathcal{L}U_n-\mathcal{N}U_n\right\|_\infty, \tag{25}$$

is less than a prescribed tolerance. In our experiments, this is chosen to be of order 10^{-15}. In (25), $\mathcal{L}$ and $\mathcal{N}$ are given by (17) or (19), depending on which iterative method is being considered, and the implementation is performed with the corresponding discrete operators described earlier.

Results of our simulations are first presented for the BO system. The computations were performed using the spatial interval $[-35,35]$. Figure 2 shows the form of the approximate profiles obtained with the Petviashvili method for the values $\gamma=0.8,\alpha=1.2$ and $c_s=0.57$. They are negative waves. An indication that the iteration is converging may be obtained by observing the eigenvalues of the iteration matrix (see Table 1). The first column shows the absolute value of the six eigenvalues of the iteration matrix having the largest magnitude, for the classical fixed-point algorithm (17) evaluated at the approximate profiles shown in Figure 2. The second column reveals the same information for the Petviashvili iteration. The first column shows the presence of the homogeneity $\lambda=2$ as the dominant

eigenvalue and the eigenvalue $\lambda = 1$ also appears. Both of these are simple. The rest of the spectrum is less than one in absolute value. The second column in Table 1 shows the spectrum of the Petviahsvili iteration. We observe that the dominant eigenvalue has been completely filtered while the rest of the spectrum is preserved. The presence of the eigenvalue $\lambda = 1$ is associated with the translational invariance of the system (7). Its only effect would be the displacement of the profiles to the right or left. This aspect can be controlled by starting with an even initial guess. One checks straightforwardly that the iteration preserves evenness, thereby obviating the possible effect of translation. As far as the e-Petviashvili method (20) is concerned, it has the same filtering effect on the spectrum as does the Petviashvili method and the leading eigenvalues of its iteration matrix are the same as those displayed in Column 2 in Table 1, to order 10^{-1}.

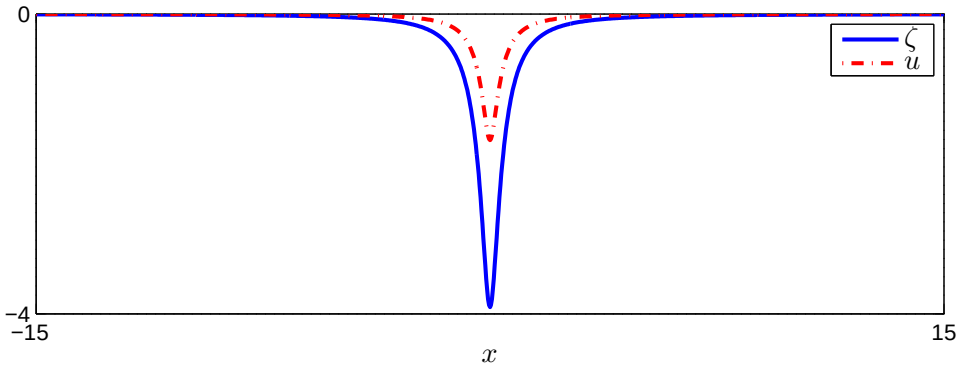

FIGURE 2. Solitary-wave solutions of the BO system. Approximate ζ and u profiles generated using the Petviashvili method (18) with $\gamma = 0.8, \alpha = 1.2$ and $c_s = 0.57$.

Classical fixed point method	Petviashvili method
1.9999999	0.9999999
0.9999999	0.8192378
0.8192378	0.6840761
0.6840761	0.6220421
0.6220421	0.5686637
0.5686637	0.5454789

TABLE 1. The six eigenvalues largest in magnitude of the iteration matrices evaluated at the profiles shown in Figure 2: (left) classical fixed point algorithm (17) and (right) the Petviashvili method (18).

The performance of the methods is further illuminated in Figures 3 and 4. Figure 3 shows in a logarithmic scale the behaviour of the stabilizing factor (see (18) and (20)) as a function of the number of iterations. If either Petviashvili method is to converge to an exact solution, it must be the case that the sequence $\{M_n\}$ approaches one. This is indeed what is observed. The algorithms are also checked by computing the residual error (25). This error has been measured as a function of the number of iterations as well as the computational time (in seconds). The

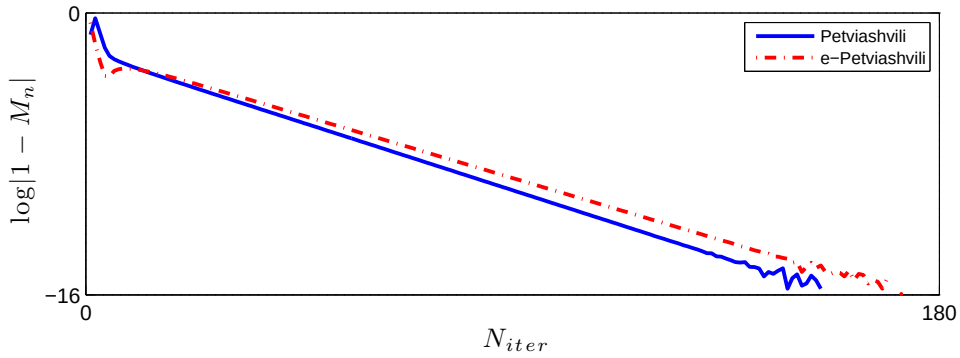

FIGURE 3. Discrepancy $|1 - M_n|$ of the stabilizing factor vs. number of iterations for the BO system using the Petviashvili-type methods (18) and (20).

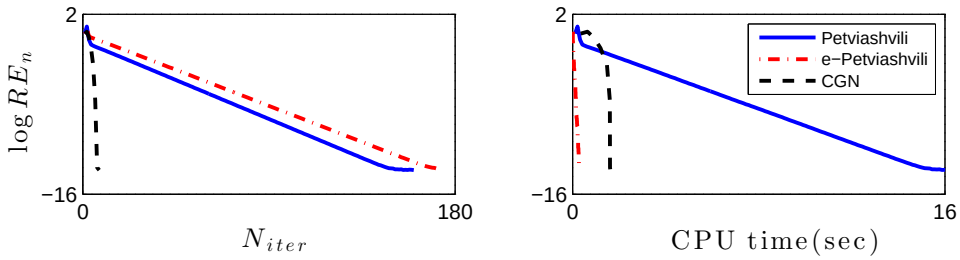

FIGURE 4. Logarithm of residual errors (25) vs. the number N_{iter} of iterations and vs. CPU time for the BO system and for the three iterative methods.

results are shown in Figure 4. As far as the number of iterations is concerned, the Petviashvili type methods give similar results while the CGN method performs much better. However, the CGN method is considerably more computationally intensive than the Petviashvili methods, owing to having to solve a nonlinear system at each iteration. The graph of computational time reveals the e-Petviashvili method to be the best in terms of accuracy achieved for effort expended.

The numerical generation of solitary waves for the ILW system presents performance properties that are, in all aspects discussed here, quite similar to those for the BO system. The conclusions about it are thus the same as those just enunciated for the BO system. Taking $\gamma = 0.8, \varepsilon = \sqrt{\mu} = 0.1$ and $\alpha = 1.2$, Figure 5 shows examples of ILW sytem solitary waves with speeds $c_s = 0.475$ and 0.52, obtained by using the Petviashvili method.

3.5. **Time dependent discretizations.** A further test of the computed solitary-wave profiles consists of measuring their accuracy as approximations of traveling-wave solutions of the time-dependent system (5). To this end, these profiles are used as initial conditions for the numerical integration of (5). The propagation of the resulting numerical solution is studied using several error indicators to be described momentarily.

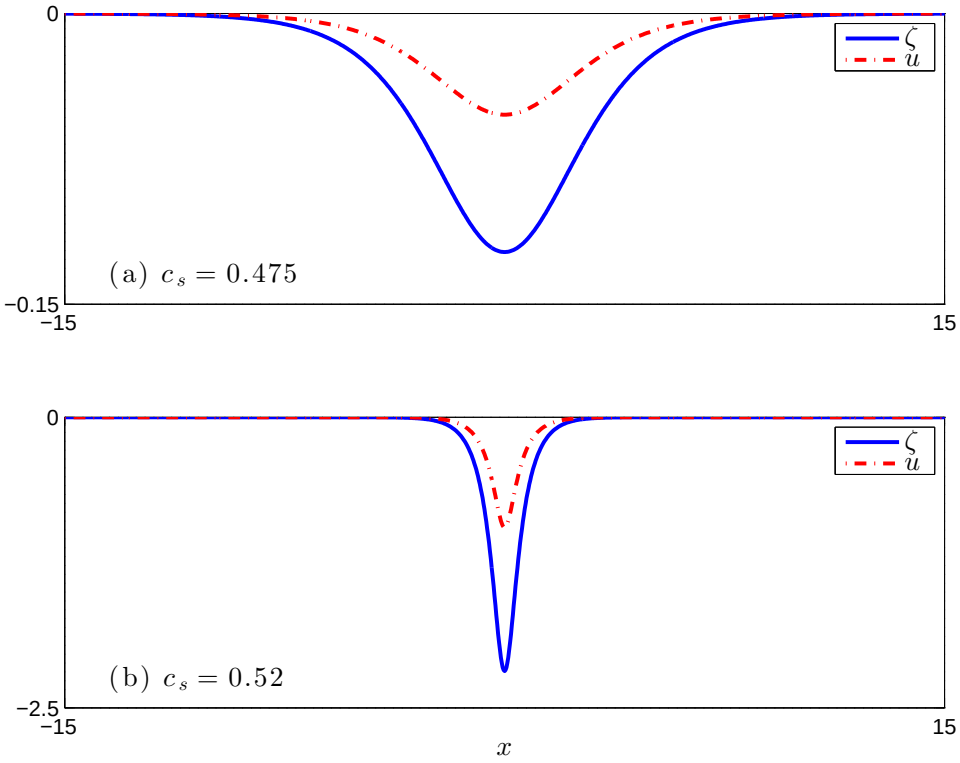

FIGURE 5. Graph of an approximate solitary-wave solution of the ILW system. The approximate profiles ζ, u were generated using the Petviashvili method (18) with $\gamma = 0.8$.

We start with a description of the numerical scheme used to approximate time-dependent solutions of the ILW and BO systems. The periodic initial-value problem for (5) on a sufficiently large spatial interval $[-\ell, \ell]$ is considered, just as for the analysis of solitary-wave solutions. After rescaling to $[-\pi, \pi]$, the problem is approximated numerically using Fourier collocation in the spatial variable. The resulting semidiscrete scheme, *cf.* [31, 50], that approximates the solution (ζ, u) of the system (5) on $[-\pi, \pi]$ by $\zeta^N, u^N \in S_N$, is defined by the Galerkin equations

$$\begin{aligned}\left\langle \left[1 + \sqrt{\mu}\tfrac{\alpha}{\gamma}\mathcal{H}\right]\zeta_t^N + \left[\tfrac{1}{\gamma}(1-\varepsilon\zeta^N)u^N - (1-\alpha)\tfrac{\sqrt{\mu}}{\gamma^2}\mathcal{H}u^N\right]_x, \chi\right\rangle = 0,\\ \left\langle u_t^N + \left[(1-\gamma)\zeta^N - \tfrac{\varepsilon}{2\gamma}(u^N)^2\right]_x, \chi\right\rangle = 0, \quad \forall \chi \in S_N,\end{aligned}$$

for $t \geq 0$, with initial data $\zeta^N(x,0) = I_N\zeta_0$, $u^N(x,0) = I_N u_0$, where I_N is the trigonometric interpolant defined for a function $h = h(x)$, say, as $I_N h(x) = \sum_{k=-N}^{N} \hat{h}_k e^{\mathrm{i}kx}$. By choosing $\chi = e^{-\mathrm{i}kx}$ for $k = -N, \cdots, N$, there obtains the initial-value problem for the system

$$\begin{aligned}\frac{d}{dt}\hat{\zeta}_k + a(k)\hat{u}_k + b(k)(\hat{\zeta} * \hat{u})_k = 0,\\ \frac{d}{dt}\hat{u}_k + c(k)\hat{\zeta}_k + d(k)(\hat{u} * \hat{u})_k = 0,\end{aligned} \tag{26}$$

of $2N+1$ ordinary differential equations for the Fourier coefficients $\hat{\zeta}_k$, $\hat{u}_k$ of ζ^N and u^N, respectively, $k=-N,\cdots,N$. Here, the initial data $\hat{\zeta}_k(0)$ and $\hat{u}_k(0)$ for the system (26) are the k^{th} Fourier coefficients of $I_N\zeta_0$ and $I_N u_0$, respectively, while $a(k), b(k), c(k)$ and $d(k)$ are the symbols of the various Fourier multiplier operators appearing in (5), namely

$$a(k)=\mathrm{i}k\frac{\gamma-(1-\alpha)\sqrt{\mu}g(|k|)}{\gamma+\sqrt{\mu}\alpha g(|k|)}, \qquad b(k)=-\mathrm{i}k\frac{\varepsilon}{\gamma+\sqrt{\mu}\alpha g(|k|)},$$

$$c(k)=\mathrm{i}k(1-\gamma), \qquad d(k)=-\mathrm{i}k\frac{\varepsilon}{2\gamma},$$

with g the symbol of the operator $\mathcal{H}$ corresponding to the rescaled problem.

The initial-value problem for the system (26) of ordinary differential equations is now discretized in time. Letting T be the final time, the constant time step is $\Delta t=T/K$ for suitably chosen values of the integer K. For each time $t_n=n\Delta t, n=1,2,\cdots K$, the approximation $(Z_n(x),U_n(x))$ of $(\zeta^N(x,t_n),u^N(x,t_n))$ are computed as an element in S_N by solving (26) using various time stepping techniques. We began with the four-step, fourth-order Runge Kutta method [29] and then compared the results with those obtained using two A-stable DIRK (diagonally implicit Runge-Kutta) methods of orders three and four. Details of these time-stepping methods can be found in [24]. We observed no significant difference in the outcome using any of these fully discrete schemes. Convergence studies not reported here were undertaken as well and showed the expected fourth-order convergence rate for the Runge-Kutta method.

By way of illustration, an approximate solitary wave with speed $c_s=0.57$ for the BO system with $\alpha=1.2$, $\gamma=0.8$ and $\varepsilon=\sqrt{\mu}=0.1$ on the spatial interval $[-32,32]$ is constructed using one of our iterative methods. The resulting profiles for ζ and u are then used as initial conditions for the time-dependent approximation just described with the time step taken to be $\Delta t=0.01$. Indeed, the solitary-wave profiles generated by all three of our iterative approximation procedures were used as initial data in the time-dependent code. There were no appreciable differences in the outcomes, so only one of them is reported here, namely the Petviashvili method (18) with $N=4096$. The profile of the ζ component of the solitary wave at $T=0$, 50 and 100 is presented in Figure 6. (Observe that the solitary wave at $t=100$ has crossed the periodic boundary and is located mainly on the negative portion of the x-axis.) Spurious oscillations of the numerical solution were not observed at any time during this time-dependent simulation. Similar results obtained for the case of the ILW system.

To investigate quantitatively the accuracy of the approximations of solitary waves using the time-dependent scheme, various measures of error were computed. The measures used here are the normalized amplitude $\{AE_n\}$, shape $\{SE_n\}$, phase $\{PE_n\}$ and speed $\{CE_n\}$ errors at time step $n, n=1,2,\cdots K$.

The amplitude error is computed by comparing, at each timestep, the initial amplitude of the approximate profile with the corresponding time-dependent amplitude of the numerical solution. These amplitudes were computed using Newton's method to find the root $x^*=x^*(t_n)$ of the equation $\frac{d}{dx}Z_n(x)=0$ near the maximum value of Z_n, as in [37]. The normalized speed error CE_n is the difference between the speed of the computed solitary wave pulse $\tilde{c}$ and the exact speed of the solitary wave c_s, i.e. $CE_n=(\tilde{c}-c_s)/c_s$. The numerical speed $\tilde{c}$ is obtained as

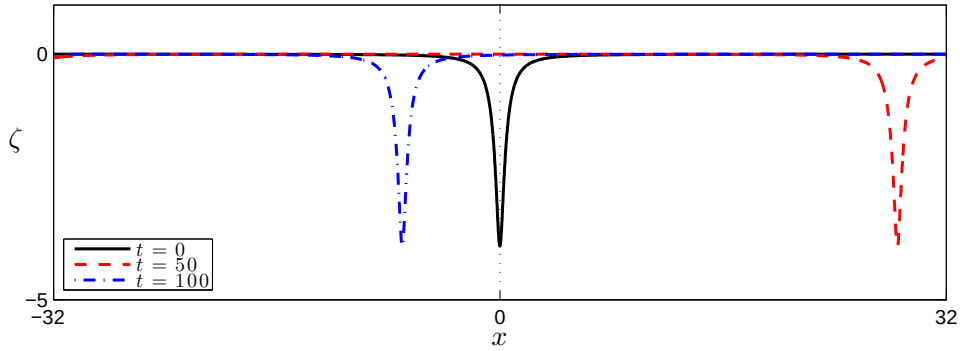

FIGURE 6. Propagation of an approximate solitary-wave solution for the BO system. The profile was generated using the Petviashvili method (18) with $c_s = 0.57$.

t^n	AE_n	SE_n	PE_n	CE_n
10	0.1091×10^{-6}	0.0768×10^{-6}	-0.0437×10^{-6}	-0.4905×10^{-8}
20	0.1256×10^{-6}	0.0871×10^{-6}	-0.0750×10^{-6}	-0.5884×10^{-8}
30	0.1356×10^{-6}	0.0932×10^{-6}	-0.1106×10^{-6}	-0.6482×10^{-8}
40	0.1431×10^{-6}	0.0974×10^{-6}	-0.1494×10^{-6}	-0.7026×10^{-8}
50	0.1492×10^{-6}	0.1007×10^{-6}	-0.1910×10^{-6}	-0.7536×10^{-8}
60	0.1546×10^{-6}	0.1035×10^{-6}	-0.2354×10^{-6}	-0.8017×10^{-8}
70	0.1596×10^{-6}	0.1059×10^{-6}	-0.2825×10^{-6}	-0.8461×10^{-8}
80	0.1642×10^{-6}	0.1081×10^{-6}	-0.3322×10^{-6}	-0.8982×10^{-8}
90	0.1686×10^{-6}	0.1101×10^{-6}	-0.3844×10^{-6}	-0.9366×10^{-8}
100	0.1728×10^{-6}	0.1121×10^{-6}	-0.4392×10^{-6}	-0.9815×10^{-8}

TABLE 2. Normalized amplitude error AE_n, shape error SE_n, phase error PE_n and speed error CE_n in the case of a solitary wave with $\gamma = 0.8, \alpha = 1.2$ and $c_s = 0.57$ for the BO system.

$$\tilde{c} = \frac{x^*(t_n) - x^*(t_{n-m})}{t_n - t_{n-m}}$$

for $n > m$. In our calculations, we chose $m = 100$. Other values of m were also tried. It did not make a lot of difference to the outcome provided m was large enough that $m\Delta t$ was of order one. The corresponding phase error is defined as $PE_n = x^*(t_n) - c_s t_n$. Finally, the L_2-based, normalized shape error SE_n is aimed at finding how well the computed solution resembles the initial data in shape, but without regard to phase. It is defined at each time step n for, lets say, the component ζ, to be

$$SE_n = \inf_{\tau} \frac{\|Z_n(x) - Z_0(x-\tau)\|_{L_2}}{\|Z_0(x)\|_{L_2}}.$$

For the computation of the shape error, the translation τ^* for which $\frac{d}{d\tau}\xi^2(\tau^*) = 0$, where $\xi(\tau) := \|Z^n(x) - Z^0(x-\tau)\|_{L_2}/\|Z_0(x)\|_{L_2}$, is computed using Newton's method and the obvious initial guess (the value of τ^* at the previous time step). The discrete shape error is the quantity $SE_n = \xi(\tau^*)$. A detailed discussion of the implementation of this type of computation is provided in [37].

Table 2 presents the amplitude, speed, shape and phase errors up to $T = 100$ for the propagation of this approximate solitary wave. This provides convincing evidence that our iterative approximations are converging to solitary-wave solutions of the relevant system.

4. **Comparisons between systems and unidirectional equations.** In this section, a comparison is undertaken of the solitary-wave solutions of the ILW and BO systems with the exact solutions of the unidirectional rBO and rILW equations. The results shown are for the BO case; results for the ILW equation are very similar. It will be seen that solitary-wave solutions of the systems and those of the unidirectional models, while not identical, are very similar in shape.

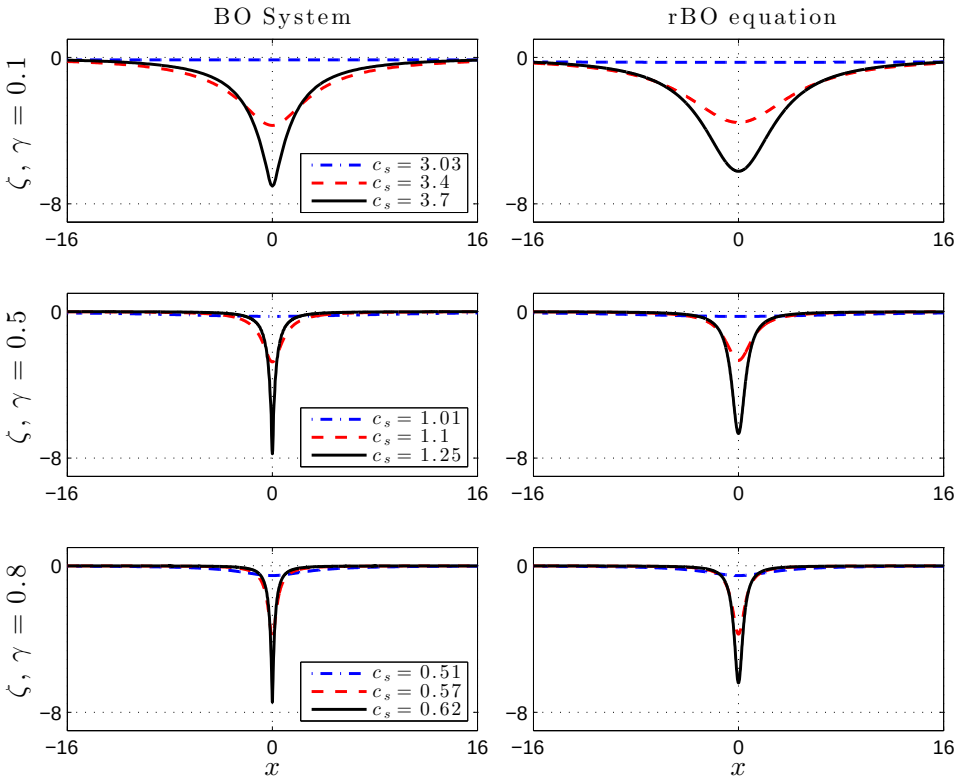

FIGURE 7. Solitary waves of the BO system (left) and the rBO equation (right) for various values of γ and c_s.

Figures 7, 9 and 10 show the computed solitary-wave profiles ζ of the BO system and rBO equation for $\alpha = 1.2$ and various values of the parameters γ and c_s. The dependence of the form of the waves on the parameter γ can be observed in Figure 7 while the dependence of the peak amplitude of the solitary waves on the speed is presented in Figure 8. For both the BO system and the rBO equation (and also for the usual version (12) with $\alpha = 0$ of the BO equation, although it is not shown here), the peak amplitude of the solitary waves increases as γ increases, which is to say that for a fixed speed c_s, the amplitude of the wave is larger when the density jump across the two homogeneous layers is smaller. In oceanic situations,

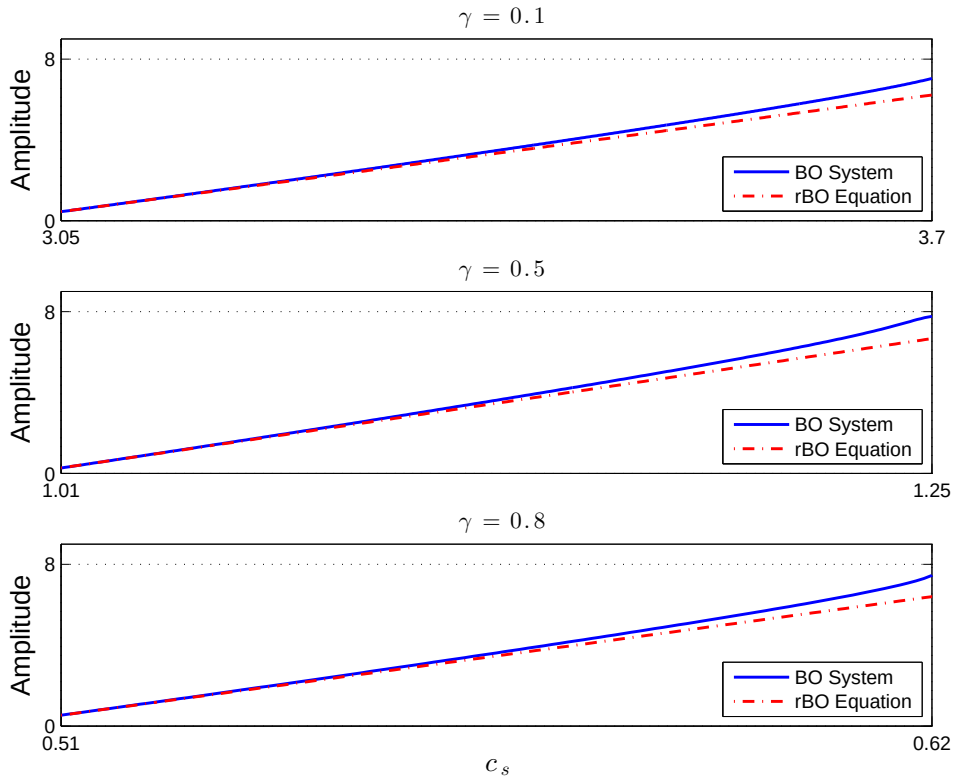

FIGURE 8. Peak amplitude of the computed solitary waves as a function of the speed c_s f or BO system and rBO equation for various values of γ.

the density jump across a pycnocline is small, so γ is quite close to one and thus the theory here would predict large amplitudes. Indeed, this is what is observed (see for example the report [8] about very large internal solitary waves in the South China Sea).

Comparing the solitary waves of the BO system and rBO equation in a little more detail, it is observed that for values of γ near 1, the two profiles very nearly agree. As mentioned, the density jump across oceanic pycnoclines is quite small, so at least as far as solitary-wave solutions are concerned, the use of the unidirectional model appears to be justified in this context.

As γ decreases, the solitary waves of the BO system becomes narrower and have slightly larger amplitude than do the corresponding solutions of rBO. This is crudely illustrated in Figures 9 and 10, corresponding to $\gamma = 0.8$ and $\gamma = 0.1$, respectively.

A final experiment was carried out to illustrate the convergence of the ILW solitary waves to those of the BO system, as the depth of the lower layer becomes indefinitely large, a fact established rigorously by Xu in [58]. This was observed for a range of the parameters in the problem, but we content ourselves with displaying one typical example in Figure 11.

5. **Conclusions.** Presented here is a computational study of the solitary-wave solutions of the ILW and the BO systems for internal wave propagation derived in

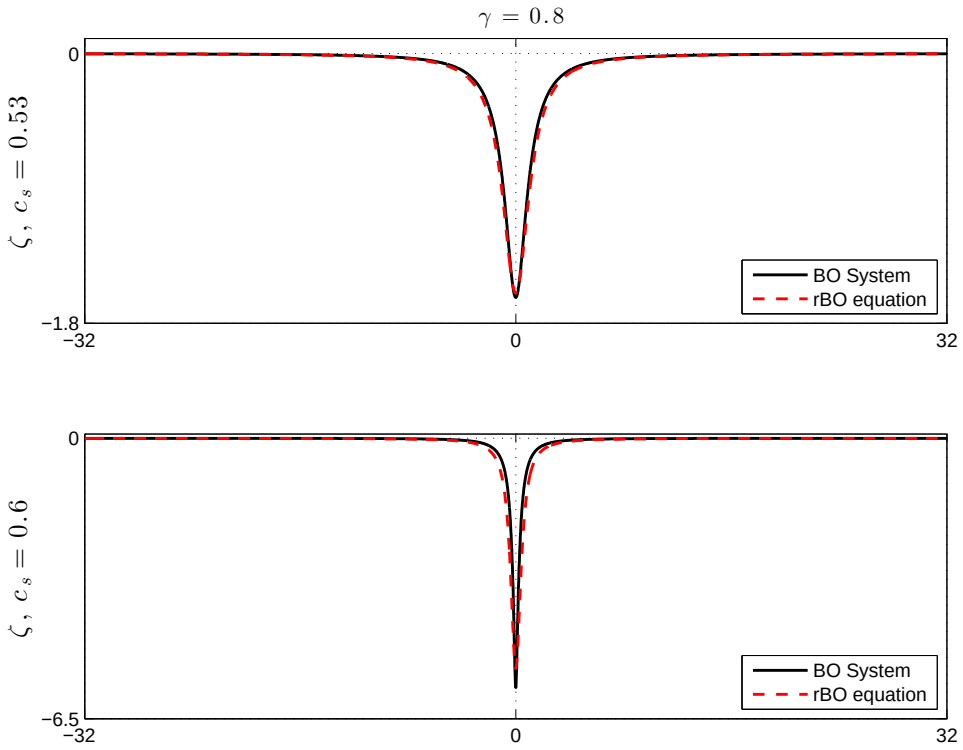

FIGURE 9. Comparison of solitary-wave solutions of the BO system and the rBO equation with $\gamma = 0.8$.

[26]. To generate appoximations of solitary-wave solutions, the relevant systems of ordinary pseudo-differential equations for the profiles are discretized and solved by a Fourier pseudospectral method on a spatial interval large enough that imposing periodic boundary conditions does not degrade the result. Three iterative techniques are applied to the corresponding discrete systems.

The results of our computations, whose accuracy is checked in Section 3, suggest that these systems possess solitary-wave solutions of all amplitues, so adding weight to the heuristic remarks made in Section 2. Comparison between solitary-wave solutions of the bi-directional systems with those of the regularized versions of the unidirectional ILW and BO models are presented in Sections 4.

Acknowledgments. JB received research support from the University of Illinois at Chicago. Part of the work on this manuscript was accomplished while he was a visiting professor in the Mathematical Sciences Department of the Ulsan Institute for Science and Technology. Some of the drafting was done during a visit to the Center for Theoretical Science at National Taiwan University. He gratefully records thanks for fine working conditions and warm hospitality at both institutions. DM and JB were supported by the Marsden Fund administered by the Royal Society of New Zealand. AD and DM were supported by the Spanish MINECO under Research Grant MTM2014-54710-P. AD was also supported by MINECO under Research Grant TEC2015-69665-R and by FEDER and Junta de Castilla y León under Research Grant VA041P17.

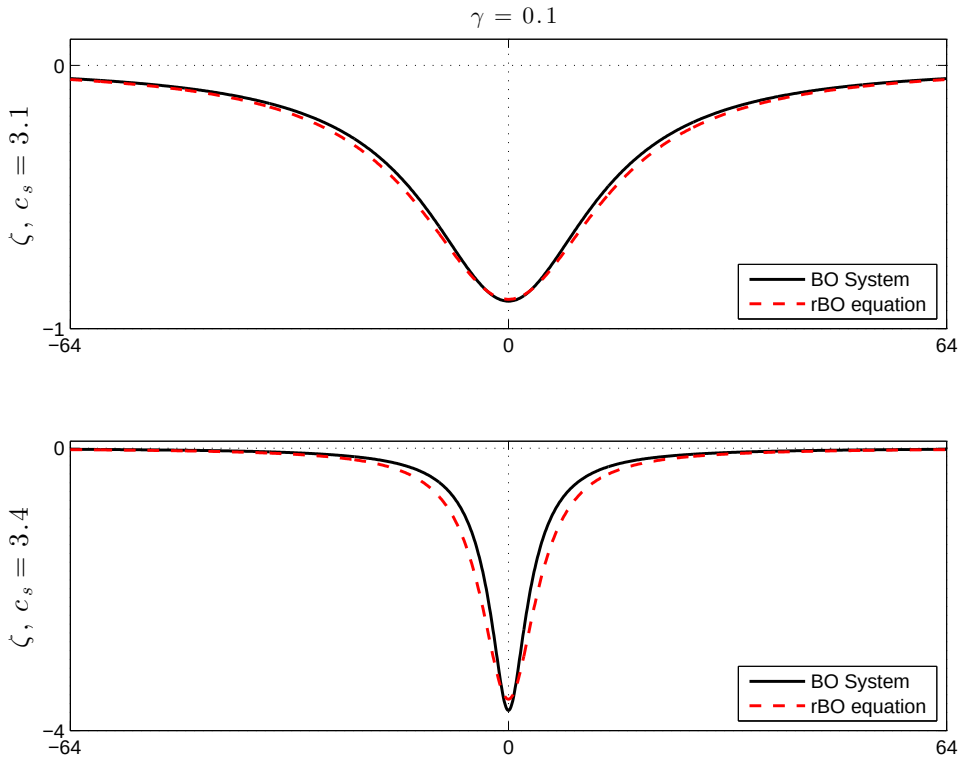

FIGURE 10. Comparison of some solitary waves of the BO system and the rBO equation with $\gamma = 0.1$.

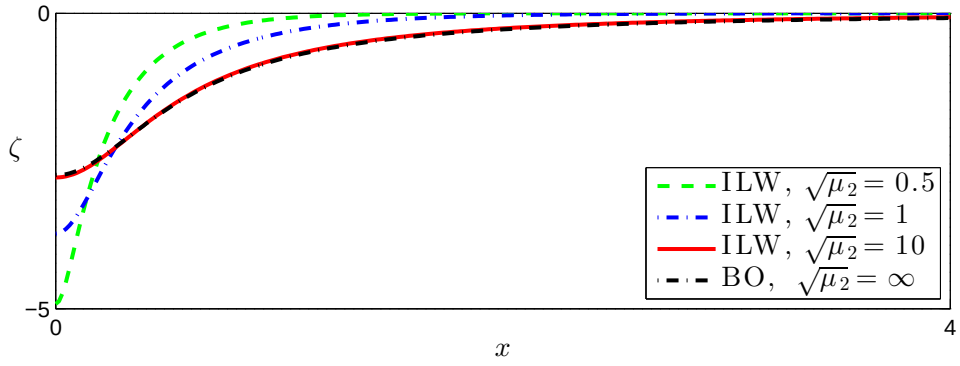

FIGURE 11. Convergence of the solitary waves of the ILW system to a solitary wave solution of the BO system for large values of the lower depth d_2; $\alpha = 1.2$, $\gamma = 0.8$, $\varepsilon = \sqrt{\mu} = 0.1$.

REFERENCES

[1] L. Abdelouhab, J. L. Bona, M. Felland and J.-C. Saut, Nonlocal models for nonlinear dispersive waves, *Physica D*, **40** (1989), 360–392.

[2] A. A. Alazman, J. P. Albert, J. L. Bona, M. Chen and J. Wu, Comparisons between the BBM equation and a Boussinesq system, *Advances Differential Eq.*, **11** (2006), 121–166.

[3] J. P. Albert and J. L. Bona, Comparisons between model equations for long waves, *J. Nonlinear Sci.*, **1** (1991), 345–374.
[4] J. P. Albert and J. L. Bona, Total positivity and the stability of internal waves in fluids of finite depth, *IMA J. Applied Math.*, **46** (1991), 1–19.
[5] J. P. Albert, J. L. Bona and J.-M. Restrepo, Solitary-wave solutions of the Benjamin equation, *SIAM J. Appl. Math.*, **59** (1999), 2139–2161.
[6] J. P. Albert, J. L. Bona and J.-C. Saut, Model equations for waves in stratified fluids, *Proc. Royal Soc. London, Series A*, **453** (1997), 1233–1260.
[7] J. P. Albert and J. F. Toland, On the exact solutions of the intermediate long-wave equation, *Differential Integral Eq.*, **7** (1994), 601–612.
[8] M. H. Alford et al., The formation and fate of internal waves in the South China Sea, *Nature*, **521** (2015), 65–69.
[9] J. Álvarez and A. Durán, An extended Petviashvili method for the numerical generation of traveling and localized waves, *Comm. Nonlinear Sci. Numer. Simul.*, **19** (2014), 2272–2283.
[10] J. Álvarez and A. Durán, Petviashvili type methods for traveling wave computations: I. Analysis of convergence, *J. Comput. Appl. Math.*, **266** (2014), 39–51.
[11] J. Álvarez and A. Durán, Petviashvili type methods for traveling wave computations: II. Acceleration with vector extrapolation methods, *Math. Comput. Simul.*, **123** (2016), 19–36.
[12] D. M. Ambrose, J. L. Bona and T. Milgrom, Global solutions and ill-posedness for the Kaup system and related Boussinesq systems, *Indiana U. Math. J*, **68** (2019), 1173–1198.
[13] C. J. Amick and J. F. Toland, Uniqueness of Benjamin's solitary wave solution of the Benjamin-Ono equation, *IMA J. Appl. Math.*, **46** (1991), 21–28.
[14] J. Angulo-Pava and J.-C. Saut, Existence of solitary waves solutions for internal waves in two-layers systems, *Quart. Appl. Math.*,, **78** (2020), 75–105.
[15] C. T. Anh, Influence of surface tension and bottom topography on internal waves, *Math. Models Methods Appl. Sci.*, **19** (2009), 2145–2175.
[16] T. B. Benjamin, Internal waves of permanent form in fluids of great depth, *J. Fluid Mech.*, **29** (1967), 559–592.
[17] T. B. Benjamin, J. L. Bona and D. K. Bose, Solitary-wave solutions of nonlinear problems, *Phil. Trans. Royal Soc. London, Series A*, **331** (1990), 195–244.
[18] T. B. Benjamin, J. L. Bona and J. J. Mahony, Model equations for long waves in nonlinear, dispersive media, *Philos. Trans. Royal Soc. London, Series A*, **272** (1972), 47–78.
[19] D. P. Bennett, R. W. Brown, S. E. Stansfield, J. D. Stroughair and J. L. Bona, The stability of internal solitary waves in stratified fluids, *Math. Proc. Cambridge Philos. Soc.*, **94** (1983), 351–379.
[20] J. L. Bona, Convergence of periodic wave trains in the limit of large wavelength, *Appl. Sci. Res.*, **37** (1981), 21–30.
[21] J. L. Bona, X. Carvajal, M. Panthee and M. Scialom, Higher-order Hamiltonian model for unidirectional water waves, *J. Nonlinear Sci.*, **28** (2018), 543–577.
[22] J. L. Bona and H. Chen, Solitary waves in nonlinear dispersive systems, *Discrete Cont. Dynamical Sys. B*, **2** (2002), 313–378.
[23] J. L. Bona, M. Chen and J.-C. Saut, Boussinesq equations and other systems for small-amplitude long waves in nonlinear dispersive media. I: Derivation and linear theory, *J. Nonlinear Sci.*, **12** (2002), 283–318.
[24] J. L. Bona, V. A. Dougalis, O. A. Karakashian and W. R. McKinney, Conservative, high-order numerical schemes for the generalized Korteweg-de Vries equation, *Philos. Trans. Royal Soc. London, Series A*, **351** (1995), 107–164.
[25] J. L. Bona, A. Durán and D. Mitsotakis, Solitary-wave solutions of Benjamin-Ono and other systems for internal waves. II. Dynamics, In preparation.
[26] J. L. Bona, D. Lannes and J.-C. Saut, Asymptotic models for internal waves, *J. Math. Pures. Appl.*, **89** (2008), 538–566.
[27] J. L. Bona and Y. A. Li, Decay and analyticity of solitary waves, *J. Math. Pures Appl.*, **76** (1997), 377–430.
[28] J. L. Bona and M. Scialom, The effect of change in the nonlinearity and the dispersion relation of model equations for long waves, *Canadian Appl. Math. Quart.*, **3** (1995), 1–41.
[29] J. C. Butcher, *The Numerical Analysis of Ordinary Differential Equations: Runge-Kutta Methods and General Linear Methods*, John Wiley & Sons, Ltd., Chichester, 1987.

[30] R. Camassa, W. Choi, H. Michallet, P.-O. Rusas and J. K. Sveen, On the realm of validity of strongly nonlinear asymptotic approximations for internal waves, *J. Fluid Mech.*, **549** (2006), 1–23.
[31] C. Canuto, M. Y. Hussaini, A. Quarteroni and A. T. Zang, *Spectral Methods in Fluid Dynamics*, Springer; New York, 1985.
[32] H. Chen, Long-period limit of nonlinear, dispersive waves: The BBM equation, *Differential Integral Eq.*, **19** (2006), 463–480.
[33] H. H. Chen and Y. C. Lee, Internal-wave solitons of fluids with finite depth, *Phys. Rev. Lett.*, **43** (1979), 264–266.
[34] W. Choi and R. Camassa, Weakly nonlinear internal waves in a two-fluid system, *J. Fluid Mech.*, **313** (1996), 83–103.
[35] W. Choi and R. Camassa, Fully nonlinear internal waves in a two-fluid system, *J. Fluid Mech.*, **396** (1999), 1–36.
[36] W. Craig, P. Guyenne and H. Kalisch, Hamiltonian long-wave expansions for free surfaces and interfaces, *Comm. Pure Appl. Math.*, **58** (2005), 1587–1641.
[37] V. A. Dougalis, A. Durán, M. A. Lopez-Marcos and D. Mitsotakis, A numerical study of the stability of solitary waves of the Bona-Smith family of Boussinesq systems, *J. Nonlinear Sci.*, **17** (2007), 569–607.
[38] V. A. Dougalis, A. Durán and D. Mitsotakis, Numerical approximation of solitary waves of the Benjamin equation, *Math. Comput. Simul.*, **127** (2016), 56–79.
[39] V. Duchene, Asymptotic shallow water models for internal waves in a two-fluid system with a free surface, *SIAM J. Math. Anal.*, **42** (2010), 2229–2260.
[40] V. Duchene, Boussinesq/Boussinesq systems for internal waves with a free surface, and the KdV approximation, *M2AN Math. Model. Numer. Anal.*, **46** (2012), 145–185.
[41] M. Frigo and S. G. Johnson, The design and implementation of fftw3, *Proc. IEEE*, **93** (2005), 216–231.
[42] P. Guyenne, D. Lannes and J.-C. Saut, Well-posedness of the Cauchy problem for models of large amplitude internal waves, *Nonlinearity*, **23** (2010), 237–275.
[43] K. R. Helfrich and W. K. Melville, Long nonlinear internal waves, *Annual Review of Fluid Mechanics*, **38** (2006), 395–425.
[44] R. I. Joseph, Solitary waves in a finite depth fluid, *J. Phys. A*, **10** (1977), L225–L227.
[45] R. I. Joseph, Comment on "internal-wave solitons of fluids with finite depth", *Phys. Rev. A*, **21** (1980), 691–692.
[46] H. Kalisch, Error analysis of spectral projections of the regularized Benjamin-Ono equation, *BIT*, **45** (2005), 69–89.
[47] H. Kalisch and J. L. Bona, Models for internal waves in deep water, *Discrete Contin. Dynamical Syst.*, **6** (2000), 1–20.
[48] C. G. Koop and G. Butler, An investigation of internal solitary waves in a two-fluid system, *J. Fluid Mech.*, **112** (1981), 225–251.
[49] T. I. Lakoba and J. Yang, A generalized Petviashvili iteration method for scalar and vector Hamiltonian equations with arbitrary form of nonlinearity, *J. Comp. Phys.*, **226** (2007), 1668–1692.
[50] B. Mercier, *An Introduction to the Numerical Analysis of Spectral Methods*, Lectures Notes in Physics, Vol. **318**, Springer-Verlag, Berlin, 1989.
[51] H. Michallet and E. Barthelemy, Experimental study of interfacial solitary waves, *J. Fluid Mech.*, **366** (1998), 159–177.
[52] H. Y. Nguyen and F. Dias, A Boussinesq system for two-way propagation of interfacial waves, *Physica D*, **237** (2008), 2365–2389.
[53] H. Ono, Algebraic solitary waves in stratified fluids, *J. Phys. Soc. Japan*, **39** (1975), 1082–1091.
[54] D. Pelinovsky and Y. Stepanyants, Convergence of Petviashvili's iteration method for numerical approximation of stationary solutions of nonlinear wave equations, *SIAM J. Numer. Anal.*, **42** (2004), 1110–1127.
[55] V. Petviashvili, Equation of an extraordinary soliton, *Sov. J. Plasma Phys.*, **2** (1976), 469–472.
[56] M. I. Weinstein, Existence and dynamical stability of solitary wave solutions of equations arising in long wave propagation, *Comm. Partial Differential Eq.*, **12** (1987), 1133–1173.
[57] G. B. Whitham, *Linear and Nonlinear Waves*, John Wiley & Sons Inc.; Hoboken, New Jersey, 1999.

[58] L. Xu, Intermediate long wave systems for internal waves, *Nonlinearity*, **25** (2012), 597–640.
[59] J. Yang, *Nonlinear Waves in Integrable and Nonintegrable Systems*, Society for Industrial and Applied Mathematics; Philadelphia, 2010.

Received October 2019; revised February 2020.

E-mail address: bona@math.uic.edu
E-mail address: angel@mac.uva.es
E-mail address: dimitrios.mitsotakis@vuw.ac.nz